Production of high-quality electron beams in numerical experiments of laser wakefield acceleration with longitudinal wave breaking

P. Tomassini,* M. Galimberti, A. Giulietti, D. Giulietti,† L. A. Gizzi, and L. Labate‡
Intense Laser Irradiation Laboratory–IPCF, Area della Ricerca CNR, Via Moruzzi 1, 56124 Pisa, Italy

F. Pegoraro
Dipartimento di Fisica, Università di Pisa and I.N.F.M Unita's di Pisa, 56124 Pisa, Italy
(Received 24 July 2003; published 30 December 2003; corrected 30 December 2003)

In 1998 Bulanov *et al.* [Phys. Rev. E **58**, R5257 (1998)] proposed a novel scheme for the production of high-quality electron beams in laser wakefield acceleration in which a controlled longitudinal nonlinear wave breaking is induced by a tailored electron density profile. This proposal was supported by both analytical and numerical results in a spatially one-dimensional configuration. In this paper we present results of a particle-in-cell simulation, two-dimensional in space and three-dimensional in the fields, of the interaction of an ultraintense laser pulse with a preformed plasma where the electron density decreases steeply from a first to a second plateau. We show that in our regime two-dimensional effects play a relevant role, allowing the production of well collimated, short and almost monochromatic electron beam. Remarkably low values of transverse and longitudinal normalized beam emittance $\epsilon^{tr}_{rms} = 9 \times 10^{-2}$ mm mrad and $\epsilon^{lon}_{rms} = 2$ mm keV are obtained.

DOI: 10.1103/PhysRevSTAB.6.121301 PACS numbers: 52.38.Kd, 52.65.Rr

I. INTRODUCTION

Laser produced plasmas are presently considered as very interesting media where charged particles can be accelerated for various applications. The electron bunches produced so far by the interaction of superintense and ultrashort laser pulses with plasmas, e.g., via laser wakefield acceleration (LWFA) [1] or self-modulated LWFA [2], are characterized by an almost 100% energy spread [3–5]. However, in most applications of laser-plasma produced electron bunches (e.g., in the electron injection in a particle accelerator [6] or in the tunable x-ray sources based on the Thomson scattering of an intense laser beam impinging on energetic electron bunches [7,8]), a reduced energy spread and a low transverse emittance of the beam are required. For this reason several teams are presently investigating, with theoretical and experimental approaches, different possibilities of reducing energy spread and beam emittance [9–13].

Adjusting the plasma density distribution so as to optimize the acceleration of an electron beam in a LWFA has been suggested and used on several occasions. The techniques proposed so far range from pulse guiding in preformed channels [14], to pulse front steepening using thin foils [15], to compensate the accelerated particle dephasing in the so-called unlimited acceleration scheme [16] and, finally, to particle injection into the pulse wakefield. Wave breaking induced by plasma inhomogeneity was proposed in Ref. [9] as a means of controlled electron injection in the wakefield of a single laser pulse. This scheme has been investigated analytically and numerically in Ref. [9] in a one-dimensional (1D) model: the wave breaking is induced by the propagation of a laser pulse in a preformed plasma with a decreasing density at the interface between two uniform regions (see also Ref. [10]), where the local decrease of the wake phase speed induces the breaking of a relatively small portion of the wake. Recently, Suk *et al.* have published a paper presenting 2D simulations in a LWFA regime with sharp density transition in tapered plasma channels [17]. In that paper the authors focused on the improvement of the final electron beam maximum energy by introducing a suitable slow increase of the longitudinal density profile after the density transition (i.e., inside the acceleration region).

In this paper we extend the analysis of the controlled injection scheme proposed in Ref. [9] by performing two-dimensional in space and three-dimensional in the fields (2.5D) particle-in-cell (PIC) simulations of the interaction between the preformed plasma and the ultrashort laser pulse. This allows us to take into account 2D effects that can enable an antagonist mechanism of wave breaking (i.e., transverse wave breaking [13,18–20]). In addition, we consider a different regime of longitudinal wave breaking, i.e., one in which the density transition scale length L is shorter than the plasma wavelength λ_p (sharp transition). We show that, with appropriate setup parameters, 2D effects do not destroy the longitudinal wave-breaking mechanism of electron injection, allowing the production of energetic electron bunches with remarkable beam quality.

This paper is organized as follows: in Sec. II the process of nonlinear wave breaking of Langmuir waves

*Email address: tomassini@ipcf.cnr.it
†Also at Dipartimento di Fisica Università di Pisa, Unità INFM, Pisa, Italy
‡Also at Dipartimento di Fisica Università di Bologna, Bologna, Italy

in 1D plasmas with inhomogeneous density is considered. In Sec. III we present the results of 2.5D particle-in-cell simulations of the interaction between an ultrashort laser pulse and a preformed plasma with a sharp density depletion. The injection of a thin bunch of particles in the accelerating phase of the Langmuir wave and its subsequent acceleration up to energies of several MeV's will be clearly identified and the production of an electron bunch with a good beam quality will be shown. Section IV will be devoted to a discussion of the numerical results.

II. WAVE BREAKING DUE TO A DENSITY DECREASE

The 1D plasma wave dynamics in the nonlinear regime can be easily described in Lagrangian coordinates in the case where the electron quiver velocity v_q is nonrelativistic [21,22]. The Euler coordinate z is related to the Lagrange coordinate z_0 through the relationship $z = z_0 + \xi(z_0, t)$. If $\beta_q \equiv v_q/c \ll 1$, the equation of motion in Lagrange coordinates of the single electrons in the plasma wave is linear in the electron displacement $\xi(z_0, t)$ which can be written as $\xi(z_0, t) = \xi_m \cos(kz_0 - \omega_{pe}t)$, where k is the plasma wave number and $\omega_{pe} = (4\pi n_e e^2/m_e)^{1/2}$ is the local plasma frequency which depends on the local electron density n_e. Here m_e and e are the electron mass and charge, respectively.

Let us consider an electron plasma wave excited by an ultrashort laser pulse of wavelength λ_l and pulse duration $\tau < 2\pi/\omega_{pe}$. Let $n_c = \pi/(r_e\lambda_l^2)$ be the plasma critical density at the laser wavelength, with $r_e = e^2/m_e c^2$ the classical electron radius, and let us suppose that the electron density is homogeneous and much smaller than the critical density ($n_e/n_c \ll 1$). In this case the plasma wave phase velocity v_{ph} is equal to the group velocity of the laser pulse v_{gl} and they can be approximately expressed as $v_{ph}/c \equiv \beta_{ph} \simeq 1 - n_e/(2n_c) \lesssim 1$. The plasma wavelength is then $\lambda_p = 2\pi/k = 2\pi v_{ph}/\omega_{pe} \simeq \lambda_l\sqrt{n_c/n_e}$. By solving the equation of motion of the electrons in Lagrangian coordinates and by performing a change of variables from Lagrange to Euler coordinates [22] an exact expression of the electric field of the (cold and 1D) plasma wave in a nonrelativistic quiver motion can be obtained:

$$a_z(z,t) = \frac{eE_z(z,t)}{mc\omega_l} = 2\frac{\omega_{pe}^2}{ck\omega_l}\sum_{n=1}^{\infty}\frac{1}{n}J_n(nk\xi_m)\sin[n(kz - \omega_{pe}t)], \quad (1)$$

where J_m is the Bessel function of the first kind and ξ_m can be estimated from the amplitude of the quiver momentum p_m:

$$\xi_m = \frac{\lambda_{pe}}{2\pi}\frac{p_m}{mc}. \quad (2)$$

In a 1D plasma, wave breaking occurs when the quiver velocity of the electrons in the Langmuir wave becomes equal to the phase velocity $v_{ph} = \omega_p/k$ of the wave [23], i.e., when the Jacobian $J(z_0, t) \equiv |\partial_{z_0} z| = |1 + \partial_{z_0}\xi_m|$ of the transformation from the Euler to Lagrangian coordinates vanishes. In a cold 1D plasma with nonrelativistic electron quivering, the wave breaking takes place when $k\xi_m = 1$.

Let us first recall the case considered in Ref. [9] of a plasma wave excited in a weakly inhomogeneous background density, with a profile consisting of two homogeneous regions with a transition characterized by a scale length L larger than the wavelength of the plasma wave. If the plasma density decreases in the direction of the pulse propagation, the wave number k increases with time and the very simple relation

$$\partial_t k = -\partial_x \omega_p \quad (3)$$

holds. The resulting decrease of the phase velocity at the interface between the two uniform density regions makes the wave break, even when its initial amplitude is below the wave-breaking threshold. As a result of the breaking at the interface between the two regions, fast electrons from the wave crest are trapped by the wave and are preaccelerated into the lower density region where the wakefield remains regular. An energy balance argument shows [9] that in this weakly inhomogeneous case the relative density of fast electrons is approximately given by the ratio $v_{ph}/(\omega_{pe}L)$ where ω_{pe} is the plasma frequency at the interface and L its inhomogeneity length.

In the actual 3D geometry an additional breaking mechanism arises from the dependence of the wakefield frequency on its amplitude, in the case of laser pulses approaching relativistical intensities. The resulting increase of the longitudinal wave number at the periphery of the laser pulse path, where the amplitude of the wakefield is smallest, bends the constant phase surfaces of the wake in a characteristic horseshoe shape [24]. This bending eventually leads to a wave breaking in the direction perpendicular to that of the pulse propagation, as discussed in Refs. [18,19,20]. This breaking regime can accelerate particles, although in an uncontrolled way, and causes a significant transverse spread of the momenta of the accelerated electrons even in the case of a transversally wide laser pulse. As a result, in order to exploit the longitudinal wave-breaking mechanism to obtain controlled electron trapping in a 3D geometry, the effects of transverse breaking of the Langmuir wave must be made negligible, i.e., the number of crests behind the pulse not involved in transverse breaking must be large [19].

III. 2.5D NUMERICAL RESULTS

A preformed plasma consisting of two quasiuniform regions with a sharp transition can be realized by exploding two properly shaped foils. Hydrodynamic simulations performed with the POLLUX code [25] indicate that tailored plasma density profiles can be realized with a target consisting of two plastic foils with different thickness and heated by a suitable pulse with duration ranging from picoseconds to nanoseconds, depending on the desired acceleration length and transition scale length [26].

We have investigated the interaction of the laser pulse with such a preformed plasma, the LWFA process and the controlled injection of particles in the acceleration phase of the wakefield with 2.5D PIC simulations. We adopted a PIC code, developed by Ruhl [27], which runs on 16 processors of a *SP*4 supercomputer at CINECA [28]. In the simulations approximately 10^8 particles move in a box of size $(40 \times 150)\ \mu\mathrm{m}^2$ sampled with 2.5×10^6 cells, corresponding to a spatial resolution of $0.05\lambda_l$. Here we present the results of a simulation in which a *p*-polarized, plane-wave pulse with Gaussian envelope, a waist size $w = 20\ \mu$m, and a time duration (full width at half maximum) $t_{\mathrm{FWHM}} = 17$ fs, an intensity $I = 2.5 \times 10^{18}\ \mathrm{W/cm^2}$ and wavelength $\lambda_l = 1\ \mu$m ($a_0 = 8.5 \times 10^{-10}\sqrt{I\lambda_l^2} \simeq 1.3$) was initialized in vacuum and impinged onto the preformed plasma. We denote the longitudinal and transverse coordinates with respect to the pulse propagation direction by z and y, respectively. After a smooth vacuum-plasma transition, the longitudinal profile of the electron density reaches a first plateau (zone I, $30\ \mu\mathrm{m} < z < 50\ \mu$m) with $n_e^{\mathrm{I}} = 2.1 \times 10^{19}\ \mathrm{cm^{-3}}$ and then it decreases abruptly with a scale length $L = 2\ \mu$m to a second plateau (zone II) $n_e^{\mathrm{II}} = 1.1 \times 10^{19}\ \mathrm{cm^{-3}}$.

The laser pulse waist w and intensity I are chosen in order to inhibit uncontrolled trapping of particles: transverse wave breaking in the homogeneous regions has been controlled by choosing both a large waist size and a relatively low pulse intensity [18,19]; in addition the square of the normalized amplitude a_0^2 of the laser pulse is well below the Lorentz factor of the Langmuir phase speed $\gamma_{ph} \simeq (n_c/n_e)^{1/2}$ so that relativistic trapping does not occur [29].

The results of the simulation confirm that bunches of particles are injected in the acceleration phase of the Langmuir wave via controlled longitudinal breaking of a portion of the wave at the interface between regions I and II. At time $t = 190$ fs a regular Langmuir wave is generated inside the first plateau [see Fig. 1(a)]. The phase-space plot [Fig. 1(b)] shows that no particle has been injected at the vacuum-plasma transition, i.e., the density profile is smooth enough to inhibit transverse wave breaking at the interface vacuum plasma (see, e.g., [13]). The maximum longitudinal momentum of the

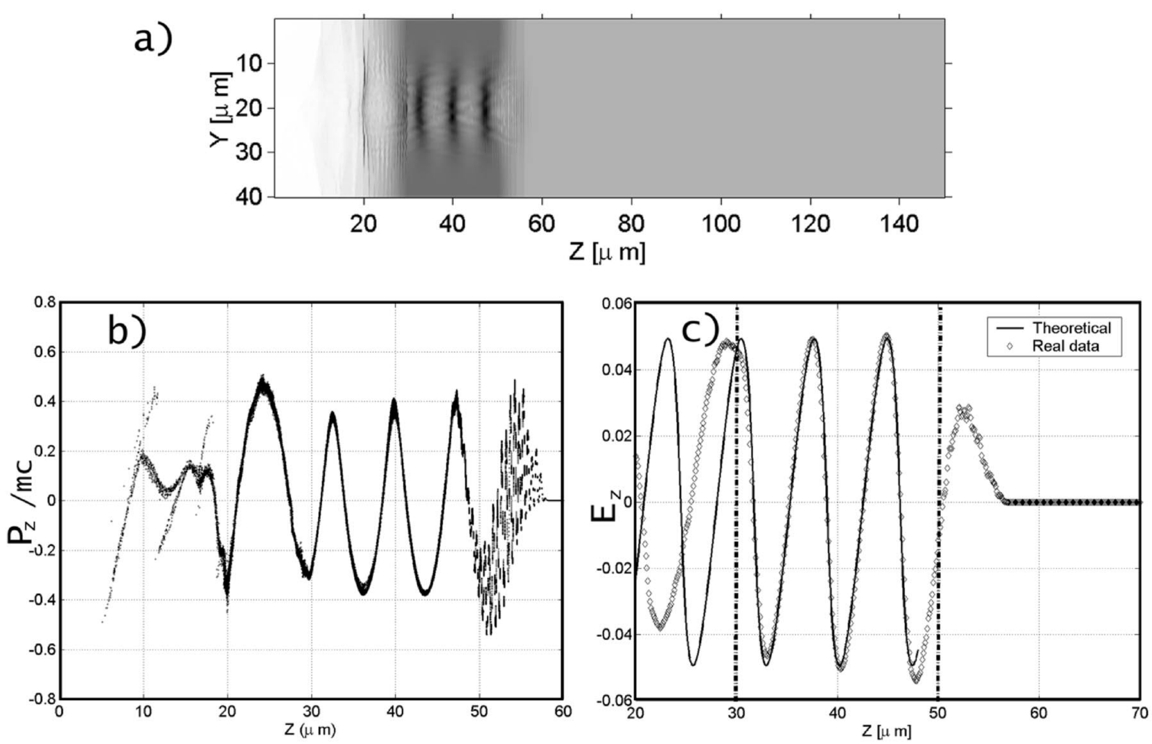

FIG. 1. (a) Electron density at $t = 190$ fs: the laser pulse peak lies at $z = 60\ \mu$m and the wakefield behind the laser pulse is well developed. (b) Lineout of the longitudinal phase-space plot $z - p_z$ on the symmetry axis. No particle has been injected. (c) Comparison between the lineout of the longitudinal electric field (marked line) and the theoretical electric field obtained from the 1D nonrelativistic model [see Eq. (1)]. As expected, the two curves agree in the region $30\ \mu\mathrm{m} < z < 50\ \mu$m where the unperturbed electron density is constant.

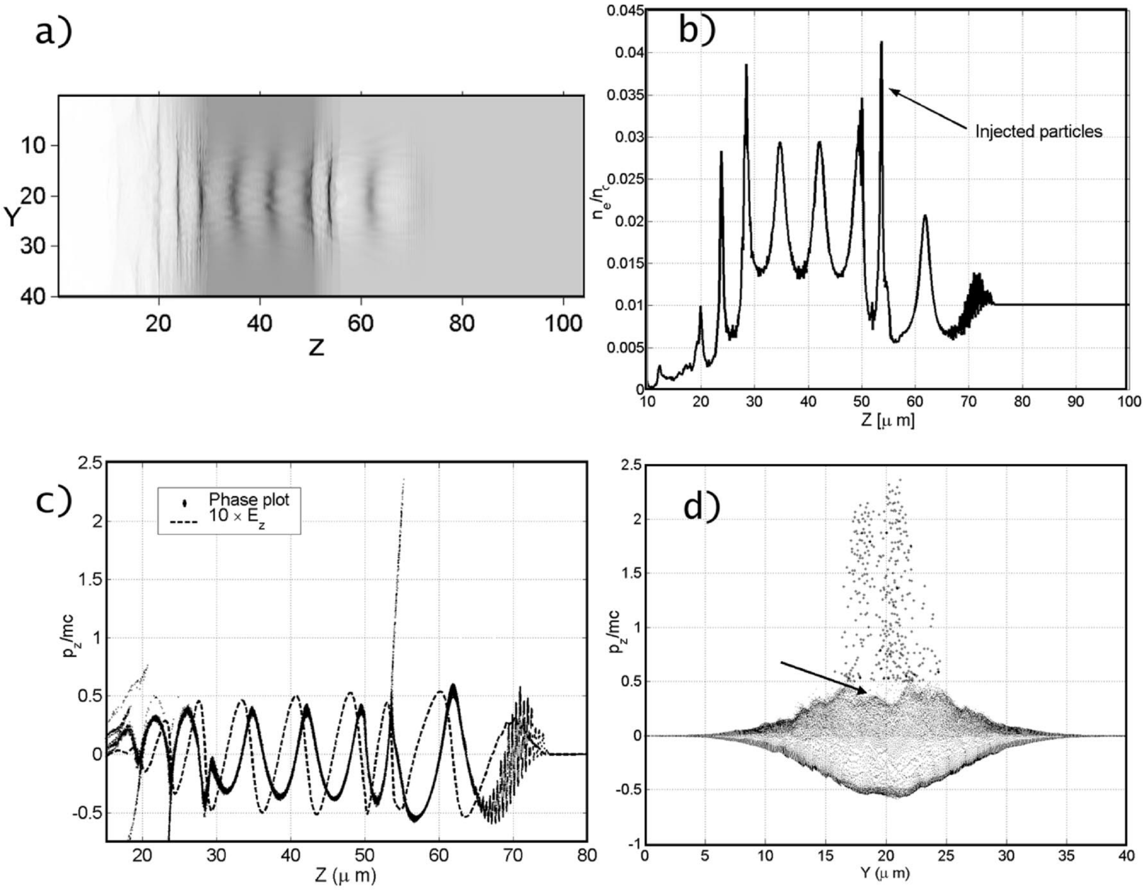

FIG. 2. $t = 250$ fs. (a) Electron density. The second crest behind the pulse is partially broken. (b) Lineout of the electron density on the symmetry axis confirming the partial breaking of the second crest and showing that the third crest is about to break. (c) Lineout on the symmetry axis of the longitudinal phase-space plot $z - p_z$ (single points) and lineout of the longitudinal electric field (dashed line). There is a factor of 10 between the two scales. The injected particles experience a negative (i.e., accelerating) electric field. (d) Cut of the $y - p_z$ phase space for 52 μm $< z <$ 55 μm. All the particles with momentum $p > 0.3mc$ have been injected in the accelerating phase. The arrow indicates the region of the phase-space plot in which the particles have been extracted from the plasma wave.

electrons of the wake inside zone I is $p_m \approx 0.4mc$, i.e., the motion of the electrons is nonrelativistic and we can apply Eq. (2) with $\lambda_p = (2\pi)v_\phi/\omega_p \approx \lambda_l(n_c/n_e^{\mathrm{I}})^{1/2}$, obtaining $\xi_m = 0.46$ μm with $\lambda_p = 7.24$ μm. This result is confirmed by the excellent agreement between the lineout of the normalized longitudinal electric field obtained from the simulation [the dots in Fig. 1(c)] and the theoretical results obtained in the case of nonrelativistic motion in the wakefield [Eqs. (1) and (2)] with $\xi_m = 0.46$ μm, $\lambda_p = 7.24$ μm. We note immediately that since $k\xi_m \approx 0.4$, the longitudinal speed of the electrons in the wake is a fraction of the phase speed of the wake and the wakefield is far from nonlinear wave breaking.

At time $t = 250$ fs (Fig. 2) the pulse is well inside the second plateau. At this time a thin bunch of injected particles is visible in the density map at the interface between zone I and zone II [see Figs. 2(a)–2(c)]. The injected particles can be clearly identified in the longitudinal phase-space plot [see Fig. 2(c)]. A cut of the transverse phase plot in the range 52 μm $< z <$ 55 μm [Fig. 2(d)] shows that almost all the particles of the wake lying in a thin region of longitudinal and transverse size about 4 μm $\times$ 20 μm and having momentum above $0.3mc$ have been injected in the accelerating phase (i.e., in a region with negative electric field) due to nonlinear wave breaking. Moreover, the injected particles experience a focusing transverse electric field (not shown here) and are suddenly focused into a spot with transverse size of few microns.

At a later time $t = 320$ fs (Fig. 3) the accelerated electron bunch has been focused into a bullet with a transverse size of about 1 μm. Also a second bunch of particles has been injected by the breaking of the crest of the wave behind the first bunch. A new crest is about to break at the density transition.

At the final time of our simulation $t = 510$ fs (Fig. 4) the electron density map shows interesting features due to 2D effects. The wake just behind the pulse has a relatively

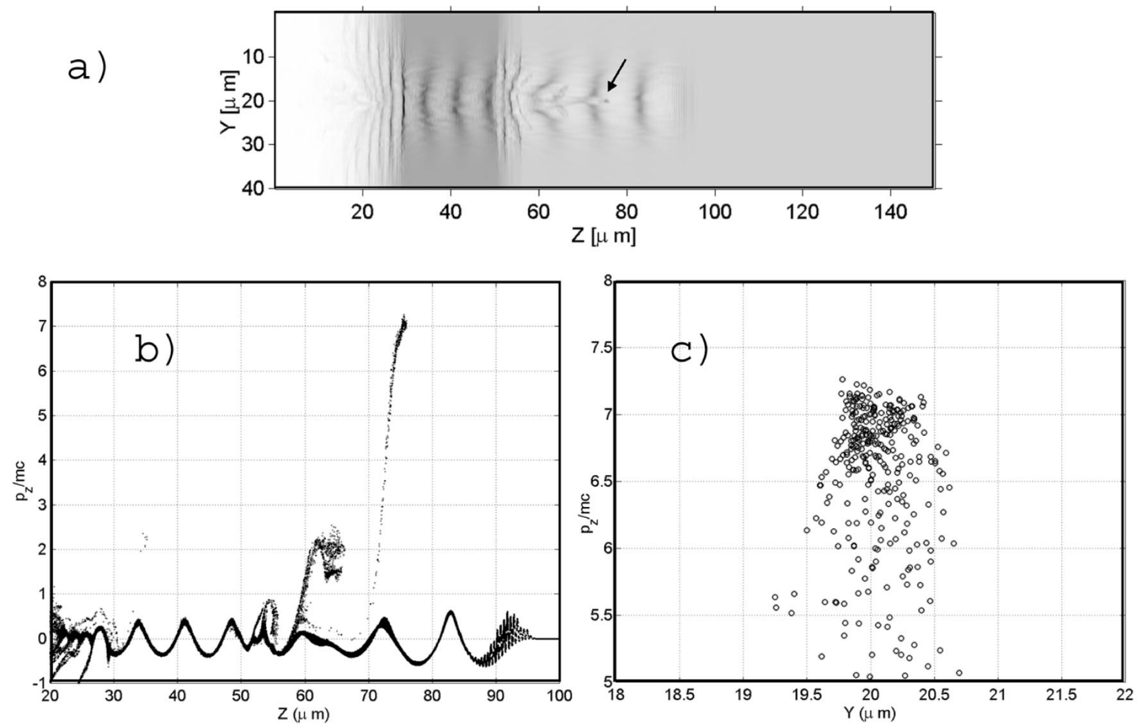

FIG. 3. $t = 320$ fs. (a) Electron density. The arrow indicates the injected bunch. (b) Lineout on axis of the longitudinal phase-space plot. The first three injected bunches are clearly visible. (c) $y - p_z$ phase-space plot of the first bunch, which has been focused into a spot size of about 1 μm by the transverse electric field.

high amplitude and exhibits a cusplike structure at the symmetry axis. Such an "inverted curvature" cannot be attributed to transverse wave breaking. In fact, the computation of the number of crests behind the pulse not broken transversally (see Eq. [5] in Ref. [19]) shows that transverse wave breaking occurs at the crests several hundred microns away from the pulse. Actually, the most probable mechanism for the production of the inverted curvature is the excitation of a secondary wave by the train of the accelerated particles [30]. Such 2D effects are responsible for the wave damping away from the laser pulse [see Fig. 4(c)]. It is interesting to note that region I is not involved in the wave damping, just because no fast particle has been generated inside it.

At the same simulation time the first electron bunch appears as a well localized bullet of $N_e = 1 \times 10^8$ particles with an energy of about 10 MeV, located in a focusing and accelerating region of the wake [see Figs. 4(a) and 4(c)]. The longitudinal phase-space plot shows that almost all the particles lie in the region of maximum accelerating force so that the bunch is still far from the defocusing limit and can still be accelerated further efficiently. The second bunch has very different characteristics, being much more distributed in both momentum and position. Moreover, the electric field experienced by the second bunch is about one-half of that accelerating the first bunch, so that the energy gap between the two bunches increases with time. We observe that these circumstances enable the possibility of selecting the first bunch simply by using a bending magnet.

The produced electron bunch is characterized by an excellent beam quality, both longitudinally and transversally. The transverse phase-space plot [see Fig. 4(b)] shows that the transverse momentum of the particles is limited to $p_y \approx 1.5mc$ and that the spatial distribution is confined into a region of transverse size $r \approx 1$ μm. The normalized rms transverse emittance $\epsilon^{\rm tr}_{\rm rms}$ gives a measure of the transverse size of the phase-space plot and it can be evaluated by computing an ensemble mean $\langle\,\rangle$ of single momentum p^i_y and position y^i of the single particles as [6] $\epsilon^{\rm tr}_{\rm rms} = (1/2mc)\sqrt{\langle y^2\rangle\langle p^2_y\rangle - \langle y p_y\rangle^2} = 9 \times 10^{-2}$ mm mrad. The longitudinal normalized rms emittance $\epsilon^{\rm lon}_{\rm rms}$ can be computed in a similar way, obtaining $\epsilon^{\rm lon}_{\rm rms} = c\sqrt{\langle \Delta z^2\rangle\langle \Delta p^2_z\rangle - \langle \Delta z \Delta p_z\rangle^2} = 2$ mm keV, where $\Delta z^i = z^i - \bar{z}$ and $\Delta p^i_z = p^i_z - \bar{p}_z$. Finally, the energy spectrum of all the accelerated particles [see Fig. 4(d)] consists of a sharp peak centered at $E = 10$ MeV (the selected electron bunch, with full width at half maximum $\Delta E_{\rm FWHM} \approx 0.5$ MeV, i.e., with a relative energy spread $\Delta E_{\rm FWHM}/E \approx 5\%$), a second peak centered at $E \approx 5$ MeV (the second bunch), and a background distribution.

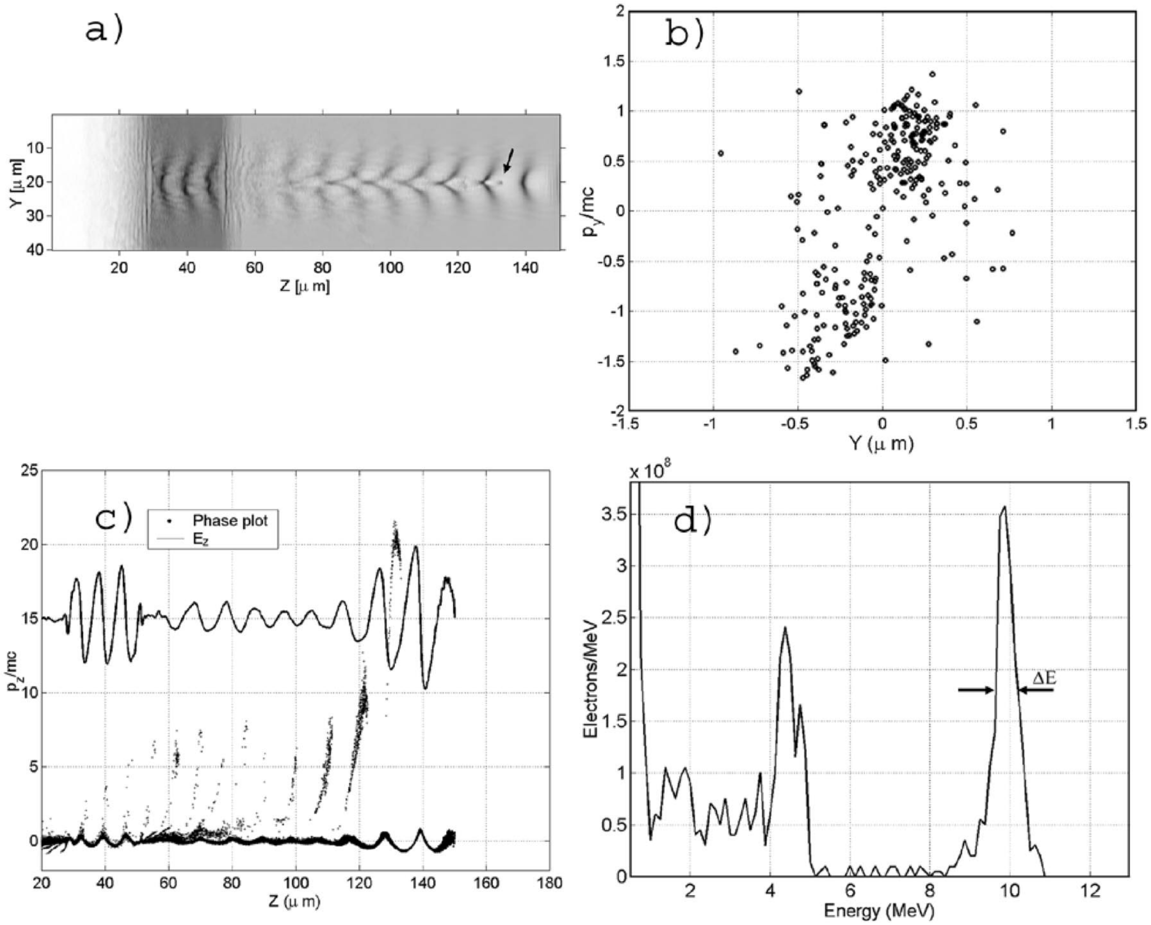

FIG. 4. $t = 510$ fs. (a) Electron density. The arrow indicates the first electron bunch. (b) Transverse ($y - p_y$) phase-space plot of the first bunch. (c) Lineout on axis of the longitudinal phase-space plot (single points) and lineout of the longitudinal electric field. Almost all the particles of the first bunch are in a region in which the accelerating force is maximum. (d) Energy spectrum of the particles accelerated with energy $E > 0.5$ MeV.

IV. COMMENTS

We have investigated the process of generation and breaking of Langmuir waves in a preformed plasma consisting of two contiguous plateaus of decreasing density using 2.5D PIC simulations. The results of the simulation reported in this paper are fully compatible with the scenario of longitudinal wave breaking of a nonlinear wakefield in which the electrons oscillate nonrelativistically.

A thin packet of particles is captured by a partial longitudinal breaking of the first crest at the density transition and is injected into the accelerating phase of the wakefield in the second plateau. These particles are then focused into a bullet with transverse size about 1 μm and are further accelerated. A second bunch is injected by the breaking of the second crest and experiences both accelerating and focusing forces that are about one-half of those acting on the first bunch. The strong reduction of the electric field of the wake with the distance from the laser pulse is likely to be due to the effect of the secondary wake generated by the trapped particles. This scenario is supported by the presence of an inverted curvature in the wave crests [30]. As a result, 2D effects enable the production of bunches with low longitudinal emittance since they allow the separation of the first bunch from the remaining components of the emitted electrons simply by using a bending magnet.

After selecting the electrons with energy exceeding 7 MeV, the resulting bunch of $N_e = 1 \times 10^8$ electrons with energy $E = 10$ MeV is characterized by a remarkably good quality and has an energy spread $\Delta E/E \approx 5\%$, transverse and longitudinal size $\delta y \approx 1$ μm, $\delta z \approx 5$ μm, respectively, and emittances $\epsilon_{\rm rms}^{\rm tr} = 9 \times 10^{-2}$ mm mrad, $\epsilon_{\rm rms}^{\rm lon} = 2$ mm keV.

We stress here that such high-quality beams are ideal for a wide range of applications, including the injection of electrons in a LINAC accelerator for the production of high energy beams (e.g., in free-electron laser (FEL) experiments which require very low emittances [6]) and the production of ultrashort pulses of x rays with linear and nonlinear Thomson backscattering [12].

ACKNOWLEDGMENTS

Authors are indebted to H. Ruhl for providing the Particle-In-Cell code. Support from CINECA High Performance Computing and from INFM Parallel Computing Initiative, as well as fruitful discussions with S.V. Bulanov, L. Serafini, and R. Numico are also greatly appreciated. This work has been partially supported by Italian M.I.U.R, Project "Metodologie e diagnostiche per materiali e ambiente."

[1] T. Tajima and J.M. Dawson, Phys. Rev. Lett. **43**, 267 (1979).
[2] N.E. Andreev *et al.*, Zh. Eksp. Teor. Fiz. **55**, 551 (1992).[Sov. Phys. JETP **55**, 571 (1992)].
[3] A. Modena *et al.*, Nature (London) **377**, 606 (1995).
[4] D. Giulietti *et al.*, Phys. Plasmas **9**, 3655–3659 (2002).
[5] C. Gahn, G. Tsakiris, A. Pukhov, J. Meyer ter-Vehn, G. Pretzler, P. Thirolf, D. Habs, and K. J. Witte, Phys. Rev. Lett. **83**, 4772 (1999).
[6] J. L. Coacolo, C. Pagani, and L. Serafini, Nucl. Instrum. Methods Phys. Res., Sect. A **393**, 430–433 (1997).
[7] E. Esarey, S. K. Ride, and P. Sprangle, Phys. Rev. E **48**, 3003 (1993).
[8] P. Catravas, E. Esarey, and W. P. Leemans, Meas. Sci. Technol. **12**, 1828–1834 (2001).
[9] S.V. Bulanov *et al.*, Phys. Rev. E **58**, R5257 (1998).
[10] H. Suk *et al.*, Phys. Rev. Lett. **86**, 1011 (2001).
[11] T. Hosokai *et al.*, Phys. Rev. E **67**, 036407 (2003).
[12] E. Esarey, R. F. Hubbard, W. P. Leemans, A. Ting, and P. Sprangle, Phys. Rev. Lett. **79**, 2682 (1997).
[13] R. G. Hemker, N. M. Hafz, and M. Uesaka, Phys. Rev. ST Accel. Beams **5**, 041301 (2002).
[14] P. Sprangle *et al.*, Phys. Rev. Lett. **69**, 2200 (1992); C. G. Durfee III *et al.*, Phys. Rev. Lett. **71**, 2409 (1993); H. M. Milchberg *et al.*, Phys. Plasmas **3**, 2149 (1996).
[15] V. A. Vshivkov *et al.*, Phys. Plasmas **5**, 2727 (1998); S.V. Bulanov *et al.*, IEEE Trans. Plasma Sci. **24**, 393 (1996).
[16] S.V. Bulanov *et al.*, Laser Physics **3**, 1078 (1993).
[17] H. Suk, C. Kim, G. H. Kim, J. U. Kim, I. S. Ko, and H. J. Lee, Phys. Lett. A **316**, 233–237 (2003).
[18] S.V. Bulanov *et al.*, Phys. Rev. Lett. **78**, 4205 (1997).
[19] S.V. Bulanov, F. Pegoraro, and J. Sakai, Nucl. Instrum. Methods Phys. Res., Sect. A **410**, 477–487 (1998).
[20] S.V. Bulanov *et al.*, in *Reviews of Plasma Physics*, edited by V. D. Shafranov (Kluwer Academic, Consultants Bureau, New York, 2001), Vol 22, p. 227.
[21] J. M. Dawson, Phys. Rev. **113**, 383–387 (1959).
[22] B. K. Shivamoggi, *Introduction to Nonlinear Fluid Plasma Waves* (Kluwer Academic, Dordrecht, 1988).
[23] A. I. Akhiezer and R.V. Polovin, JETP **3**, 696 (1956); T. Katsouleas and W. Mori, Phys. Rev. Lett. **61**, 90 (1988).
[24] S.V. Bulanov *et al.*, Phys. Rev. Lett. **74**, 710 (1995).
[25] G. J Pert, J. Comput. Phys. **43**, 111–117 (1981).
[26] P. Tomassini *et al.* (to be published).
[27] H. Ruhl, "Collective Super-Intense Laser Plasma Interaction," University of Darmstadt, 2000.
[28] High Performance Systems Division of CINECA, http://www.cineca.it/HPSystems/
[29] S.V. Bulanov, V. I. Kirsakov, and A. S. Sakharov, JETP Lett. **53**, 565 (1991).
[30] T.V. Lisekina, F. Califano, V. A. Vshivkov, F. Pegoraro, and S.V. Bulanov, Phys. Rev. E **60**, 5991–5997 (1999).